

## Fabrication and photoluminescence of InGaN-based nanorods fabricated by plasma etching with nanoscale nickel metal islands

H. W. Huang, J. T. Chu, T. H. Hsueh, M. C. Ou-Yang, H. C. Kuo, and S. C. Wang

Citation: *Journal of Vacuum Science & Technology B* **24**, 1909 (2006); doi: 10.1116/1.2221317

View online: <http://dx.doi.org/10.1116/1.2221317>

View Table of Contents: <http://scitation.aip.org/content/avs/journal/jvstb/24/4?ver=pdfcov>

Published by the AVS: Science & Technology of Materials, Interfaces, and Processing

---

### Articles you may be interested in

[Spontaneous formation of InGaN nanowall network directly on Si](#)

*Appl. Phys. Lett.* **102**, 173105 (2013); 10.1063/1.4803017

[Coupling of InGaN/GaN multiquantum-wells photoluminescence to surface plasmons in platinum nanocluster](#)

*Appl. Phys. Lett.* **95**, 111112 (2009); 10.1063/1.3224176

[InN nanocolumns grown by plasma-assisted molecular beam epitaxy on A-plane GaN templates](#)

*Appl. Phys. Lett.* **94**, 221908 (2009); 10.1063/1.3151824

[Nanoscale structure fabrication of multiple Al Ga Sb In Ga Sb quantum wells by reactive ion etching with chlorine-based gases toward photonic crystals](#)

*J. Vac. Sci. Technol. B* **24**, 2291 (2006); 10.1116/1.2348727

[Improvement of microstructural and optical properties of GaN layer on sapphire by nanoscale lateral epitaxial overgrowth](#)

*Appl. Phys. Lett.* **88**, 211908 (2006); 10.1063/1.2207487

---

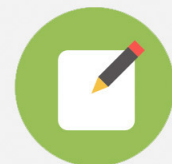


## Re-register for Table of Content Alerts

Create a profile.



Sign up today!



# Fabrication and photoluminescence of InGaN-based nanorods fabricated by plasma etching with nanoscale nickel metal islands

H. W. Huang,<sup>a)</sup> J. T. Chu, T. H. Hsueh, M. C. Ou-Yang, H. C. Kuo, and S. C. Wang  
*Department of Photonics and Institute of Electro-Optical Engineering, National Chiao Tung University,  
Hsinchu 300, Taiwan, Republic of China*

(Received 27 April 2005; accepted 15 June 2006; published 10 July 2006)

InGaN-based nanorods with a rod density of  $\sim 3.0 \times 10^{10} \text{ cm}^{-2}$  were fabricated from a light-emitting diode structure by an inductively coupled plasma dry-etching with nanoscale nickel metal islands. The nanoscale nickel metal islands were formed from a Ni film by a rapid thermal annealing at 850 °C for 1 min. The influence of thicknesses of Ni metal film on the diameter and density of nanorods was also investigated. Structural and optical properties of the InGaN-based nanorods were studied with field-emission scanning electron microscopy, transmission electron microscopy, and photoluminescence. The diameters and heights of nanorods were estimated to be 60–100 nm and more than 0.28  $\mu\text{m}$ , respectively. The emission-peak wavelength of nanorods showed a blueshift of 5.1 nm from that of the bulk structure. An enhancement by a factor of five times in photoluminescence intensity of nanorods compared to that of the bulk structure was also observed in this work. The blueshift is attributed to the strain relaxation in the well, quantum-confinement effect, or a combination of the two, which result in the enhancement in emission intensity. © 2006 American Vacuum Society. [DOI: 10.1116/1.2221317]

## I. INTRODUCTION

InGaN-based nitride semiconductors have attracted much attention for applications in the optoelectronic devices and high-temperature/power electronic devices in the visible light region.<sup>1</sup> In particular, InGaN/GaN multiple quantum wells (MQWs) are being used as the active layers for optical devices such as light-emitting diodes (LEDs) and laser diodes (LDs).<sup>2–4</sup> Recently, due to the rapid development of nanostructure fabrication methods, optical and electronic properties have been studied for potential applications on optoelectronic devices such as quantum cryptography, quantum information, and nano-light-emitting devices. For nanoscale nitride structures, until now, several nitride nanostructures have been produced by various fabrication methods, such as inductively coupled plasma reactive-ion etching (ICP-RIE) without a mask,<sup>5</sup> synthesis using carbon nanotubes as templates,<sup>6</sup> and the growth of single-crystal GaN nanorods by hydride vapor-phase epitaxy.<sup>7</sup> However, all of these reported methods are relatively complicated, and their structures without active layers are not quite appropriate for optoelectronic device applications. It has been demonstrated that it is possible to form nanometer-sized nickel (Ni) islands by choosing the correct initial Ni thickness, annealing temperature, and annealing time.<sup>8</sup> In this article, we present a method to fabricate high-density InGaN/GaN MQWs nanorods by an ICP-RIE dry-etching technique with nanoscale Ni metal islands. The structural and optical properties were examined with field-emission scanning electron microscopy (FESEM), transmission electron microscopy (TEM), and photoluminescence (PL).

<sup>a)</sup>Author to whom correspondence should be addressed; electronic mail: stevenhuang@truelight.com.tw

## II. EXPERIMENT

The LED wafers were grown by an atmospheric-pressure, two-flow, metal-organic chemical vapor deposition (MOCVD) system on *c*-axis sapphire substrates. The substrates were initially treated in H<sub>2</sub> ambient at 1100 °C for thermal cleaning; then a 30 nm thick GaN nucleation layer was grown at 550 °C. Five periods of InGaN/GaN MQWs with a photoluminescence wavelength of  $\sim 451.9$  nm were grown after growing a 3  $\mu\text{m}$  thick silicon-doped GaN layer on the nucleation layer at 1150 °C. Finally a 0.1  $\mu\text{m}$  thick magnesium (Mg)-doped GaN layer was grown on top of the InGaN/GaN MQWs at a high temperature. The estimated In composition of 0.15 was determined by x-ray diffraction (XRD).

The processing flowchart for the InGaN/GaN MQWs nanorods is shown in Fig. 1. First, a 300 nm thick SiN thin film was deposited on the samples by a plasma-enhanced chemical-vapor deposition (PECVD) system, followed by the electron-beam evaporation of a Ni metal film. Then a rapid thermal annealing (RTA) at 850 °C for 1 min under a nitrogen ambience to produce nano-sized Ni metal islands on the SiN film surface. It should be noted here that the annealing time of 1 min was performed for sufficient energy to ensure that all Ni metal islands were isolated. An RIE was conducted to etch the SiN film using a gas-mixture condition of CF<sub>4</sub>/O<sub>2</sub> to transfer the patterns of nano-size Ni metal islands down to the SiN layer. Therefore, the Ni/SiN pillars were fabricated as a nanomask following the etching process. The samples were then etched down to the *n*-type GaN layer by ICP-RIE (SAMCO ICP-RIE 101iPH) using a gas mixture condition of Cl<sub>2</sub>/Ar=50/20 sccm with a ICP source power, a bias power set at 400/100 W, and a chamber pressure of

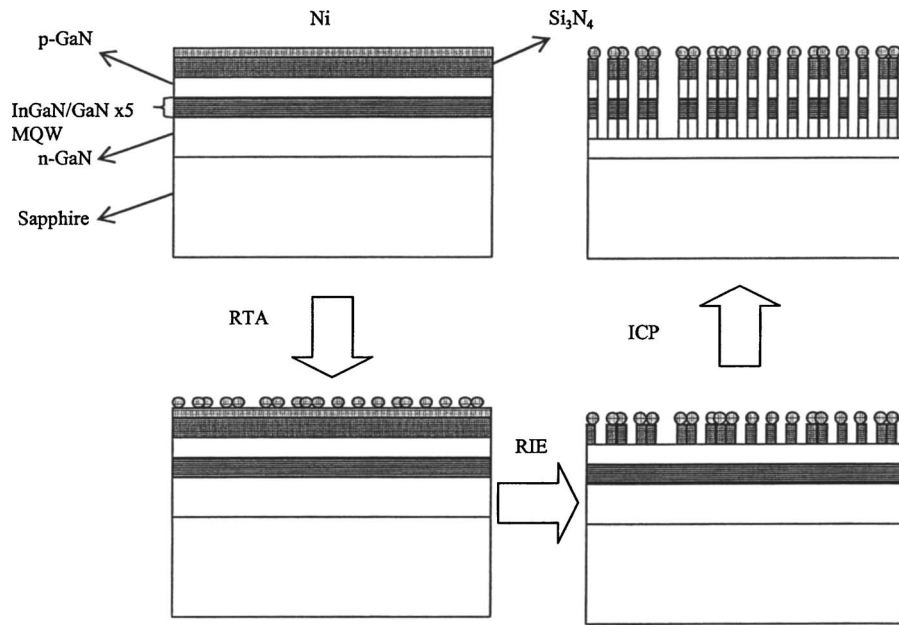


FIG. 1. Schematic processing flow-chart for the InGaN/GaN MQWs nanorods.

5 mTorr for 3 min of etching time. Finally, the Ni/SiN pillars were removed by a buffer oxide etchant to expose the InGaN/GaN MQWs nanorods.

After all these processes, the dimension and density of the InGaN/GaN MQWs nanorods were measured by the FESEM (Hitachi FE-SEM S-5000) and TEM. The optical properties were studied by PL measurements at room temperature. Samples were excited by a 325 nm He–Cd laser line with an excitation power of 25 mW and the emitted luminescence light was collected through a 0.32 m spectrometer with a charge-coupled device (CCD) detector. The best spectral resolution of this measurement system is about 1 nm with a 300 grooves/mm grating.

### III. RESULTS AND DISCUSSION

We estimate the mean dimension and density of the GaN-based nanorod LEDs as a function of the RTA temperature, as shown in Fig. 2. However, the operation RTA temperature condition under 700 °C was unable to form the Ni nanoislands. The nanorods density was estimated to be around  $2\text{--}3 \times 10^9 \text{ cm}^{-2}$  and there are no obvious changes on nanorod densities as the RTA temperature increases from 800 °C to 900 °C with a 150 Å thick Ni film. The diameter of nanorods was about 120–220 nm as the RTA temperature ranged from 800 °C to 900 °C. It has been reported that the thickness of the initial metal film can play an important role in determining surface morphology at a given annealing temperature.<sup>11,12</sup> Thus, we examined the influence of using several different thicknesses of initial Ni metal film of 50, 100, and 150 Å to investigate this effect. The mean diameter and density of nanorods as a function of thicknesses of initial Ni metal film were shown in Fig. 3. It is noted that the isolated Ni nanoislands could form for all samples with different thickness of initial Ni film at a RTA condition of 850 °C for 1 min examined from surface morphology measurements. In Fig. 3, with an increasing thickness of the ini-

tial Ni metal film from 50 to 150 Å, the nanorods density decreased from  $3 \times 10^{10}$  to  $2.2 \times 10^9 \text{ cm}^{-2}$  and the nanorod mean diameter increased from 60 to 150 nm. The origin of a decrease in nanorod density may be due to an increase in the dimension of Ni metal islands as the initial Ni metal layer increases, resulting in an increase in the mean dimension of nanorods.

As shown in the SEM images of Fig. 4(a), of Ni/SiN nanomask images, the diameter of Ni/SiN etching masks were  $\sim 200/150 \text{ nm}$  and Ni cluster height was  $\sim 100 \text{ nm}$ . The SEM image of InGaN-based nanorods fabricated by the ICP-RIE dry etching with Ni metal nanoislands is shown in Fig. 4(b). In the radial direction, the nanorods exhibited a circular geometry indicating an isotropic, homogeneous etch. A rod number density of nanorods is in the order of  $\sim 3.0$

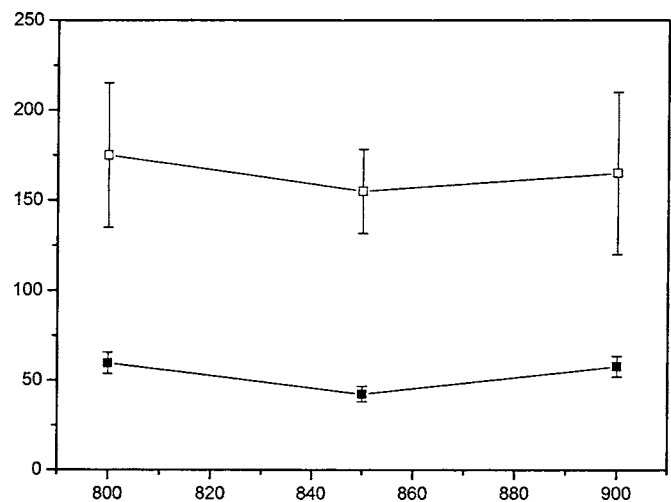


FIG. 2. Mean dimension and rod number density of InGaN-based nanorods as a function of the RTA temperature varied from 800 °C to 900 °C for 1 min with  $\text{Cl}_2/\text{Ar}$  flow rate of 50/20 sccm, ICP/bias power of 400/100 W, and a chamber pressure of 5 mTorr for 3 min of etching time.

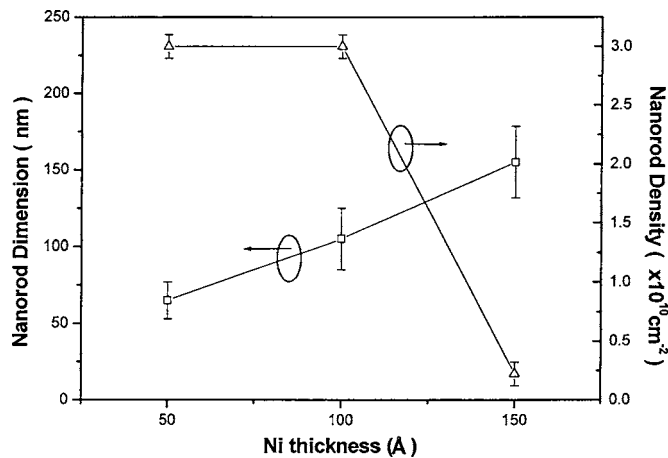


FIG. 3. Mean dimension and rod number density of InGaN-based nanorods as a function of thicknesses of initial Ni metal film from 50 to 150 Å.

$\times 10^{10} \text{ cm}^{-2}$  with a mean lateral dimension range from 60 to 100 nm, depending on the diameter of nanomasks on the nanorod. The nanorods distribute randomly, as well as the random distribution of Ni metal nanomasks. A typical TEM (JEOL, JEM-200CX) image of a single nanorod is illustrated in Fig. 5. It clearly shows that the five-period MQWs were evidently observed within the nanorod body from the TEM image. The widths of the well and barrier are

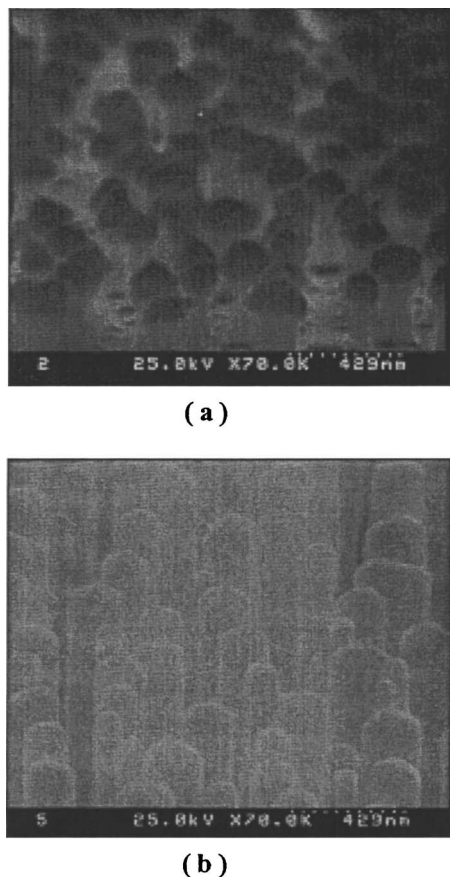


FIG. 4. Scanning electron microscope image of InGaN-based nanorods fabricated by ICP-RIE dry-etching with self-assembled Ni metal nanoislands.

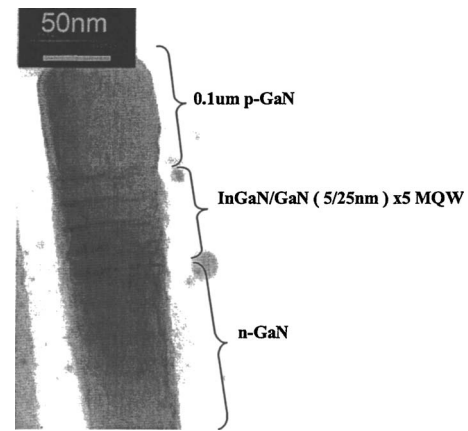


FIG. 5. Transmission electron microscopy image of a single InGaN-based nanorod.

estimated to be around 5 and 25 nm according to the growth design. The nanorod is more than  $0.28 \mu\text{m}$  in length as examined from the TEM image, indicating a high aspect-ratio etch. The nanorod has a larger diameter at the top than at its bottom, and its sidewalls were sloped and slightly rough. We attribute the imperfect sidewalls and lateral dimension to mask erosion and ion damage during the dry-etch processing. Taking the room-temperature lattice constant of Ni to be  $3.52 \text{ \AA}$  and that of the corresponding crystalline SiN surface to be  $7.61 \text{ \AA}$  in the  $a$ -direction and  $2.91 \text{ \AA}$  in the  $c$ -direction yields room-temperature strains of  $\epsilon_{a(\text{SiN/Ni})} = -53\%$  and  $\epsilon_{c(\text{SiN/Ni})} = 21\%$ , respectively. This means that the deposition of Ni on SiN results in a large degree of compression in the  $a$ -direction and tensile strain in the  $c$ -direction. Therefore, the formation of isolated Ni nanoislands on the SiN surface was performed during a thermal treatment, which was similar to the result in Ref. 8.

Figure 6 compares the normalized PL spectra from the bulk structure and the InGaN-based nanorods measured at

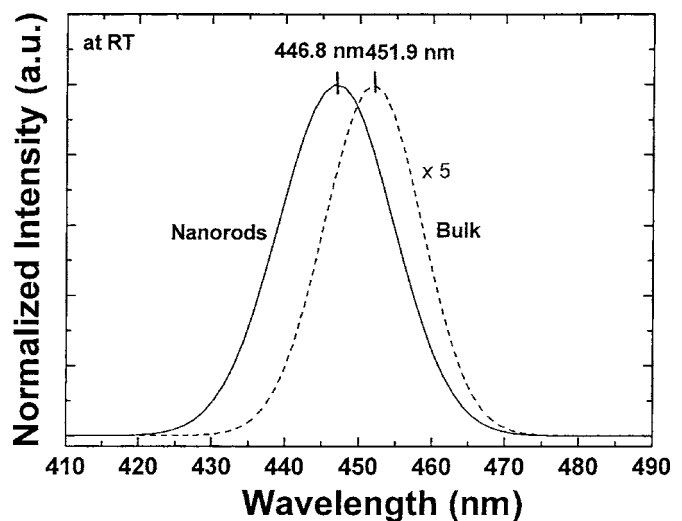


FIG. 6. Comparing the normalized PL spectra from the bulk structure and the InGaN-based nanorods excited by a He-Cd laser at room temperature.

room temperature. The PL spectra cover the spectral range from 410 to 490 nm. The excitation power density was  $1.5 \text{ W/cm}^2$  in both cases. The dominant-emission peak wavelengths for the bulk structure and the nanorods are 451.9 and 446.8 nm, respectively. A blueshift of 5.1 nm in the peak wavelength of the nanorods in the PL spectra has been observed (compared to the bulk structure sample). The blueshift can be attributed to the strain relaxation in the well,<sup>11</sup> quantum confinement effect,<sup>7,12</sup> or a combination of the two. It has been proposed that piezoelectric fields due to a mismatch-induced strain in  $\text{In}_{1-x}\text{Ga}_x\text{N}/\text{GaN}$  QWs. In the presence of the piezoelectric field, the electron and hole wave function separate spatially, leading to a reduced overlap and a reduced recombination rate. The results in Ref. 13 showed that strain relaxations were observed in GaN pillars with diameters of  $1 \mu\text{m}$  and less. Hence, our 60–100 nm nanorods should experience a strain relaxation in the well. The amount of the reduced piezoelectric field can be estimated to be around  $31.5 \text{ meV}/5 \text{ nm}=0.063 \text{ MV/cm}$ , where 5 nm is the well thickness. In addition, the PL intensity in the nanorods is enhanced by a factor of about five times that of the bulk emission. The enhancement could be due to the better overlap of the electron and hole wave functions with a reduced piezoelectric field, and an increase of the radiative recombination rate. The light scattering off the etched sidewalls and increases of surface area of the nanorods could also increase the PL intensity.

#### IV. CONCLUSION

InGaN-based nanorods with diameters of 60–100 nm and a height of more than  $0.28 \mu\text{m}$  have been fabricated by ICP-RIE dry etching with Ni metal nanoislands. The PL peak wavelength of nanorods was located at 446.8 nm and showed a blueshift of 5.1 nm from that of the bulk structure. The blueshift may be due to the strain relaxation in the QWs, quantum confinement effect, or a combination of the two. The enhancement in emission intensity of the nanorods by a

factor of five times compared to the bulk emission was observed in this work, due to the better overlap of the electron and hole wave functions, with a reduced piezoelectric field and an increase of the radiative recombination rate. The light scattering off the etched sidewalls of nanorods could also increase the PL intensity. The use of the present fabrication method should be applicable for fabricating InGaN-based nano-light-emitting devices.

#### ACKNOWLEDGMENTS

This work was supported in part by the National Science Council of the Republic of China (ROC) in Taiwan under Contract No. NSC92-2120-M-009-006 and by the Academic Excellence Program of the ROC Ministry of Education under Contract No. NSC93-2752-E-009-008-PAE.

<sup>1</sup>S. Nakamura, *Science* **281**, 956 (1998).

<sup>2</sup>T. Mukai, M. Yamada, and S. Nakamura, *Jpn. J. Appl. Phys., Part 1* **38**, 3976 (1999).

<sup>3</sup>S. Nakamura, M. Senoh, S. Nagahama, N. Iwasa, T. Yamada, T. Matsushita, H. Kiyoku, and Y. Sugimoto, *Jpn. J. Appl. Phys., Part 2* **35**, L74 (1996).

<sup>4</sup>I. Akasaki, S. Sota, H. H. Sakai, T. Tanaka, M. Koike, and H. Amano, *Electron. Lett.* **32**, 1105 (1996).

<sup>5</sup>C. C. Yu, C. F. Chu, J. Y. Tsai, H. W. Huang, T. H. Hsueh, C. F. Lin, and S. C. Wang, *Jpn. J. Appl. Phys., Part 1* **41**, 910 (2002).

<sup>6</sup>W. Q. Han, S. S. Fan, Q. Q. Li, and Y. D. Hu, *Science* **277**, 1287 (1997).

<sup>7</sup>H. M. Kim, D. S. Kim, T. W. Kang, Y. H. Cho, and K. S. Chung, *Appl. Phys. Lett.* **81**, 2193 (2002).

<sup>8</sup>J. D. Carey, L. L. Ong, and S. R. P. Silva, *Nanotechnology* **14**, 1223 (2003).

<sup>9</sup>C. Bower, O. Zhou, W. Zhu, D. J. Werder, and S. Jin, *Appl. Phys. Lett.* **77**, 2767 (2000).

<sup>10</sup>S. Aggarwal, S. B. Ogale, C. S. Ganpule, S. R. Shinde, V. A. Novikov, A. P. Monga, M. R. Burr, R. Ramesh, V. Ballarotto, and E. D. Williams, *Appl. Phys. Lett.* **78**, 1442 (2001).

<sup>11</sup>L. Dai, B. Zhang, J. Y. Lin, and H. X. Jiang, *J. Appl. Phys.* **89**, 4951 (2001).

<sup>12</sup>X. Duan, J. Wang, and C. M. Lieber, *Appl. Phys. Lett.* **76**, 1116 (2000).

<sup>13</sup>R. W. Martin, P. R. Edwards, H. S. Kim, K. S. Kim, T. Kim, I. M. Watson, M. D. Dawson, Y. Cho, T. Sands, and N. W. Cheung, *Appl. Phys. Lett.* **79**, 3029 (2001).